Effect of rare earth addition on {10$\bar{1}$2} twinning induced hardening in magnesium

Aidin Imandoust, Christopher D. Barret, Haitham El Kadiri

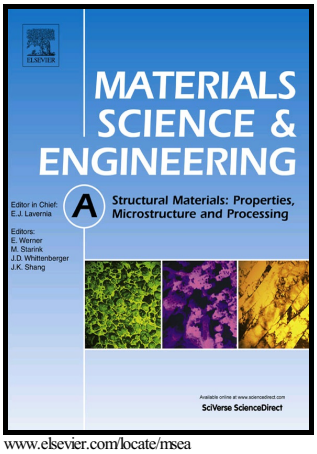

www.elsevier.com/locate/msea

PII: S0921-5093(18)30275-2
DOI: https://doi.org/10.1016/j.msea.2018.02.067
Reference: MSA36154

To appear in: *Materials Science & Engineering A*

Received date: 26 December 2017
Revised date: 15 February 2018
Accepted date: 16 February 2018

Cite this article as: Aidin Imandoust, Christopher D. Barret and Haitham El Kadiri, Effect of rare earth addition on {10$\bar{1}$2} twinning induced hardening in magnesium, *Materials Science & Engineering A*, https://doi.org/10.1016/j.msea.2018.02.067

Effect of rare earth addition on $\{10\bar{1}2\}$ twinning induced hardening in magnesium

Aidin Imandoust[a], *Christopher D. Barret*[b,c], *Haitham El Kadiri*[*,b,c]

[a] *Department of Mechanical Engineering, Auburn University, Auburn, AL, USA*

[b] *Department of Mechanical Engineering, Mississippi State University, Mississippi State, MS 39762, USA*

[c] *Center for Advanced Vehicular Systems, Mississippi State University, Mississippi State, MS 39762, USA*

Abstract

We investigated the effect of Gd and Ce additions in magnesium on sigmoidal hardening behavior associated with $\{10\bar{1}2\}$ twinning after extrusion. Compression along extrusion direction revealed that rare earth additions enhance the flow stress, while $\langle c+a\rangle$ softening was expected. This phenomenon has been explained by the enhancement of $\langle c+a\rangle$ dislocations activity and the ensuing increase in forest hardening due to solute drag. It is expected that dislocation transmutation of basal to prismatic will be enhanced during $\{10\bar{1}2\}$ twin growth in rare earth containing alloys, which would exacerbate $\langle c+a\rangle$ entanglement with the dislocation forests inside the twins. Forest hardening events overcompensated for the softening effects from lowering the critical resolved shear stresses of $\langle c+a\rangle$ dislocations, and resulted in higher flow stress for the binary rare earth containing alloys.

Keywords: magnesium; rare earth, electron backscattering diffraction (EBSD), work hardening, extension twinning

* Corresponding author
Email: elkadiri@me.msstate.edu (Haitham El Kadiri)

1. Introduction

Traditional magnesium (Mg) alloys are known to exhibit poor formability at ambient temperature due to an effect associated with profuse twinning as all easy slip systems have their burgers vector lying only on the basal plane [1, 2]. $\{10\bar{1}2\}$ twinning mode in Mg has smaller critical resolved shear stress (CRSS) than $\langle c+a\rangle$ dislocations, which have threshold stresses an order of magnitude higher for temperatures below 180 ºC [1, 2]. Hence, profuse $\{10\bar{1}2\}$ twinning takes place at low temperatures whenever deformation imposes plastic stretching along the $\langle c\rangle$-axis. However, because of the polarity of this twin mode pyramidal $\langle c+a\rangle$ slip triggers to accommodate plastic compression or contraction along $\langle c\rangle$-axis[1]. $\{10\bar{1}1\}$ twins could also trigger to provide $\langle c\rangle$-axis compression or contraction but their threshold stress is much higher than that of pyramidal $\langle c+a\rangle$ slip.

The profuse activity of $\{10\bar{1}2\}$ twinning is known to cause a boost in the hardening rate of HCP metals by orders of magnitude, but more particularly in Mg as the parent grain can be entirely consumed by this twin mode [3]. This results in a sigmoidal-shaped flow of the stress-strain behavior in sharply textured wrought alloys undergoing compression normal to the main $\langle c\rangle$-axis fibers [4-6]. When the stress sign is inverted (asymmetry) for the same loading direction or vice-versa (anisotropy), $\{10\bar{1}2\}$ twinning is remarkably obviated in these sharp fibers. However, ductility remains unimproved. It has been suggested that $\{10\bar{1}2\}$ only ensues $\{10\bar{1}1\}$ twins (i.e. double twinning), which have been shown to be detrimental to ductility as they can turn into cracks shortly after their nucleation [7, 8]. Additions of rare earth (RE) elements in Mg and its alloys have been shown to noticeably reduce anisotropy/asymmetry and ameliorate ductility. Several effects have been mentioned but there is a general consensus on texture weakening effects [9, 10]. In fact, RE enhances the formation of recrystallized grains which substantially deviate from the ideal fiber orientation after rolling or extrusion, making them less prone to twinning [2]. Nevertheless, $\{10\bar{1}2\}$ twinning is unequivocally active at room temperature (RT) [11], and its hardening effects play a significant role in RT formability of Mg-RE alloys. In this paper, in an effort to study the effect of RE additions on the role of $\{10\bar{1}2\}$ twinning in hardening, we designed experiments to favor the activity of this twinning mode. In this respect, we hampered recrystallization by exploiting process variables in order to produce samples of Mg-RE alloys with sharp $\langle 10\bar{1}0\rangle$ fiber texture. Hence, $\{10\bar{1}2\}$ twinning was equally

active during compression along extrusion direction in pure Mg and Mg-RE alloys. We monitored and investigated the effect of RE additions in high purity Mg on the $\{10\bar{1}2\}$ twinning behavior and its subsequent effects on strain hardening and plastic flow behavior.

2. Experimental procedures

Mg- 0.40 Ce, Mg- 0.51 Ce, Mg- 0.38 Gd and Mg-2.51 wt. % Gd binary alloys along with pure Mg were cast using 99.9% pure magnesium and 99.8% pure RE elements in a vacuum induction melt furnace using a tantalum crucible at Ames Laboratory. The as-cast alloys were solution treated at 450 ºC for 10 h under flowing argon gas atmosphere followed by water quenching. The chemical compositions of annealed billets were analyzed using the inductively coupled plasma atomic emission spectroscopy (ICP-AES) method. Solution treated alloys along with pure Mg were machined to cylindrical specimens ~32 mm (1.25 in) in diameter and ~25 mm (1 in) long cylinders and were subject to indirect extrusion at ram speeds of 10 mm/min at 450 ºC with extrusion ratio of 1:6 followed by air cooling. We conducted slow extrusions with small ratio in order to impose less strain energy, which is essential to drive dynamic recrystallization (DRX), and preserve the deformation texture (i.e $\langle 10\bar{1}0\rangle$ fiber) in RE-containing alloys. Therefore, we were able to trigger the formation of $\{10\bar{1}2\}$ twinning by compressing along extrusion direction (ED) (i.e. normal to $\langle c\rangle$ axis of $\langle 10\bar{1}0\rangle||ED$ grains). This emboldened the effect of $\{10\bar{1}2\}$ twinning induced hardening on the plastic flow behavior, making it clearly observable for pure Mg and Mg-RE alloys with different RE contents. Cylindrical compression samples with height to diameter ratio of 1.5 were machined from extrudates. We conducted compression tests with constant strain rate of 0.001 s^{-1} at room temperature up to true strains of 0.02, 0.04, 0.06, 0.09 and till fracture. Each test was repeated three times to be obtain statistically significant results.

Compressed samples were cut along the compression axis and prepared by standard metallographic techniques and polished using 0.06 µm colloidal silica (Struers OPS) for 10 minutes. Grain size measurement was conducted along and perpendicular to ED using OIM analysis software by EDAX. The DRX volume fraction and the size of deformed grains for Mg-RE alloys were very close and comparable. In preparation for electron back scattered diffraction (EBSD) analysis, electro-polishing was conducted using a Struers LectroPol-5 on polished samples in chilled Struers C1 electrolyte at 25 V for 120 s at -5 ºC. Samples were sonicated for

20 minutes afterwards in absolute ethanol to remove artifacts from the surface. Texture and microstructure analysis were conducted on transverse cross-sectional using EBSD. EBSD analyses were performed using a field emission scanning electron microscope (SEM) Zeiss Supra 40 at the operating voltage of 20 kV. Scanning step size was 1 µm for micro-texture measurements and 0.1 µm for ones used for intragranular misorientation axes (IGMA) analysis.

3. Results and discussions

Figure 1 shows the inverse pole figures (IPFs) of the extruded materials. RE additions retard DRX in Mg-RE alloys [12], and hence, they retain their deformed microstructure after slow extrusions with relatively smaller volume fractions of DRX grains (Table 1). This established bimodal microstructures in the extruded alloys, which are composed of deformed and DRX grains (Figure 1f). The bimodal grain size information and DRX volume fraction of extrudates are listed in Table 1. Deformed and recrystallized grains were differentiated by choosing the grain orientation spread (GOS) values smaller than 2 º for DRX grains, and the remaining for deformed grains. Higher fraction of deformed grains resulted in strong $\langle 10\bar{1}0 \rangle$ fiber texture as RE driven texture modification occurs during recrystallization [13, 14].

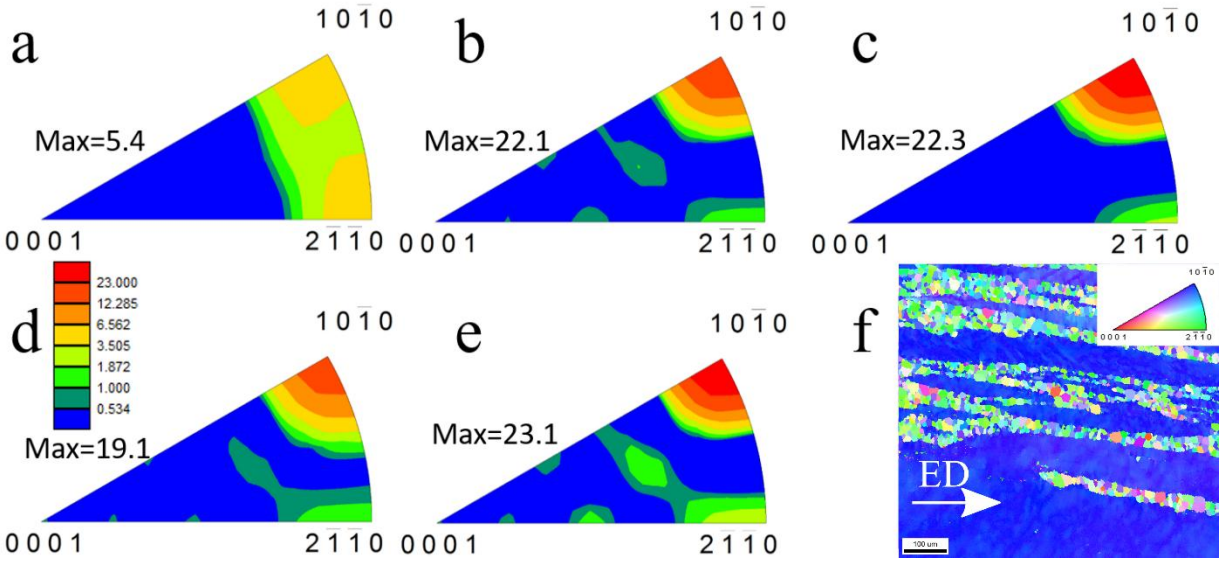

Figure 1. Inverse pole figures (IPFs) of extruded **a)** pure Mg, **b)** Mg-0.40 Ce, **c)** Mg-0.51 Ce, **d)** Mg-0.38 Gd, **e)** Mg-2.51 wt. %Gd, **f)** ED mapped IPF map of Mg-2.51 Gd as a representative initial microstructure. Extrusions were conducted at 450 ºC with 10 mm/min ram speed with 1:6 extrusion ratio.

The extensive activation of $\{10\bar{1}2\}$ twinning during compression along the ED in deformed grains of Mg-RE alloys overshadowed the contribution of DRX grains to plasticity, as the mechanical response of the samples appeared to be "Mg's typical sigmoidal behavior". Pure Mg expressed ~58 % DRX volume fraction that spread $\langle 10\bar{1}0\rangle$ fiber to $\langle 10\bar{1}0\rangle - \langle 11\bar{2}0\rangle$ fiber due to high mobility of $\{13\bar{4}0\}$ twin boundary upon recrystallization, which weakens the texture intensity [15]. However, all the grains within $\langle 10\bar{1}0\rangle - \langle 11\bar{2}0\rangle$ fiber are susceptible to $\{10\bar{1}2\}$ twinning during compression along ED, as they have their $\langle c\rangle$-axis perpendicular to ED and compression direction. Therefore, sigmoidal flow behavior during compression along ED was expected.

Table 1. Grain size data of the extruded materials obtained from low magnification EBSD scans.

Metal/Alloy (wt. %)	Grain Size (GS)-μm	Deformed GS-μm	Recrystallized GS-μm	DRX Volume Fraction (%)
High Purity Mg	41±5	-	-	58±5
Mg-0.40Ce	19±2	47±4	17±2	14±2
Mg-0.51Ce	14±2	40±3	12±2	13±2
Mg-0.38Gd	33±4	48±5	31±4	36±4
Mg-2.51Gd	16±2	48±4	14±2	33±3

Compression along ED direction, which triggered extensive formation of $\{10\bar{1}2\}$ twins, illustrated a notable difference between pure Mg and binary Mg-RE alloys regarding their $\{10\bar{1}2\}$ twinning induced hardening in Figure 2b. The higher strain hardening rate for RE-containing alloys resulted in greater maximum flow stresses in Figure 2a. On the other hand, it reduced ductility. The IPF maps of interrupted pure Mg compression samples (inset micrographs in Figure 2a) explain the plastic flow behavior in regions I-III. Region I starts after the yield point associated with activation of $\{10\bar{1}2\}$ twinning till $\varepsilon_t = 0.06$. RE addition slightly altered the work hardening rate and the flow stress in Region I (Figure 2). These minor differences may be justified by RE solute effects and grain size effects, which failed to exhibit a systematic trend [16, 17]. In other words, strengthening mechanisms such as solute strengthening, grain size refinement, RE segregation to the grains boundaries and precipitation hardening (for Mg-Ce

alloys) seemed to be overshadowed by extreme activity of $\{10\bar{1}2\}$ twinning and its interaction with lattice defects, like dislocations [3].

Meanwhile, twinning stress is directly affected by the chemical composition and grain size, the effect of which was observed in the compressive yield stress of the samples [18-20]. Since the yield strength is directly associated with the onset of twinning under the present circumstances, we take it as a qualitative criterion for twinning stress. Considering the similar grain size, structure and DRX volume fraction of RE containing alloys, the remarkable increase in yield stress with increasing RE content (see Figure. 2a) may be attributed to the solute strengthening effects. Pure Mg samples on the other hand had different grain size and structure, which made it hard to draw any solid conclusion regarding its twinning stress compared to the binary alloys. However, we expect it to have a smaller twinning stress compared to other alloys as it has less distorted/stressed lattice due to its purity, which may play a part in its lower work hardening rate [21].

At total strain of 0.06 (i.e. $\varepsilon_t = 0.06$), relatively higher volume fraction of $\{10\bar{1}2\}$ twins (crystallographically hard orientations) and immense interaction of $\{10\bar{1}2\}$ twin boundaries with basal and $\langle c+a \rangle$ dislocations increase the work hardening rate and starts Region II ($\varepsilon_t = 0.06 - 0.09$) [4, 5]. It is worth noting that $\{10\bar{1}2\}$ twinning reorients parent grains by ~86º around $\langle 11\bar{2}0 \rangle$ [22], and align their $\langle c \rangle$ axis nearly parallel to extrusion/compression direction. Hence, twinned grains (i.e. hard orientations) "*absorb a large fraction of the load*" [23], which is mainly accommodated by $\langle c+a \rangle$ dislocations [4]. Variants of $\{10\bar{1}2\}$ twins grow to saturation at $\varepsilon_t \cong 0.08$, which is commensurate with the steep increase in work hardening rate in Figure 2b. This is consistent with the consensus on traditional Mg alloys, which demonstrates the triviality of RE effects on twin growth rate [3, 4].

Although all the experimental materials express sigmoidal plastic flow behavior, the work hardening rate in region II appears to be considerably higher for Mg-RE alloys, as higher RE concentrations lead to higher work hardening rates in samples with similar grain size and structure (Figure 2b). As mentioned above, plastic deformation continues by glide of $\langle c+a \rangle$ dislocations within the twinned hard orientations in Region II [4]. It has been well understood that RE additions facilitates $\langle c+a \rangle$ slip by decreasing its CRSS value [24, 25], which results in easier dislocation glide and faster dislocation generation and multiplication [26, 27]. As a matter

of fact, higher flow stress of Mg-RE alloys insinuates that forest hardening effects may overshadow the RE-induced $\langle c+a \rangle$ softening. This effect is remarkable particularly after $\varepsilon_t = 0.08$ that commensurate with $\{10\bar{1}2\}$ twin saturation strain (Figure 2b).

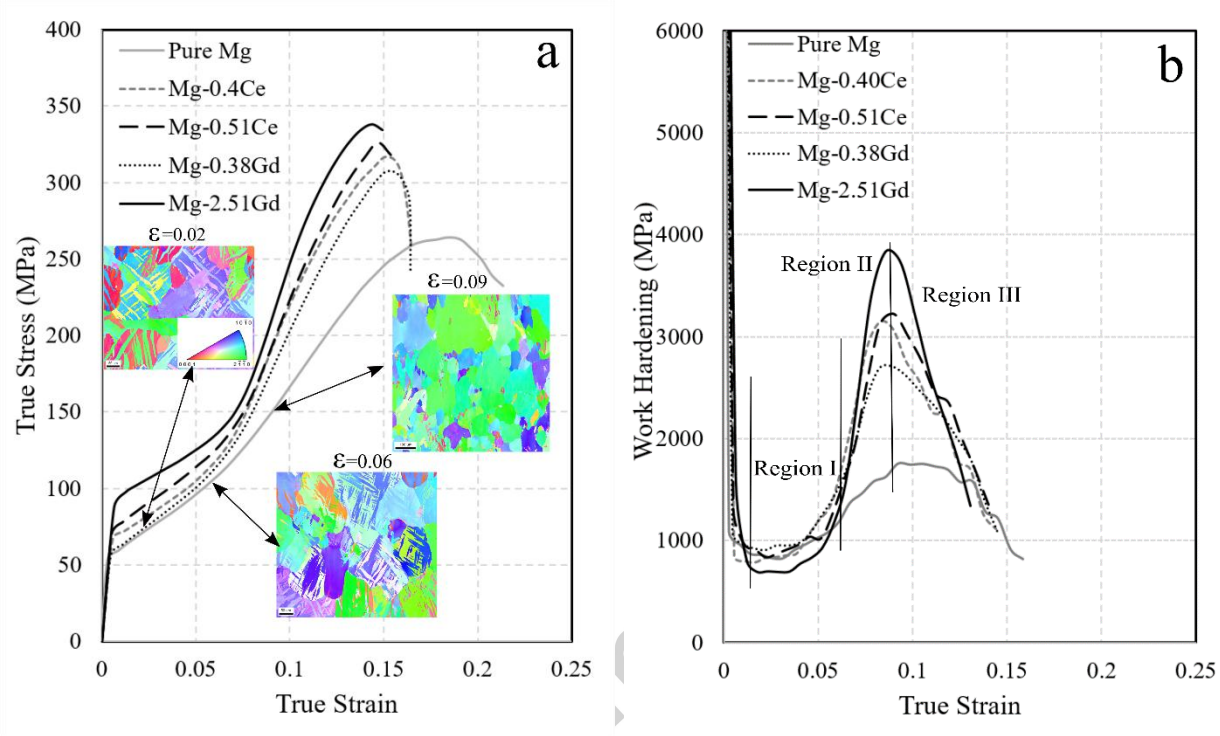

Figure 2. a) Typical true stress-true strain plot for compression tests along extrusion direction for extruded materials listed in Figure 1. The inset IPF maps correspond to pure magnesium strained to 0.02, 0.06 and 0.09 compressive true strain. **b)** The corresponding work hardening curves.

Here, the influence of solute drag on dislocation dynamics and preferential RE segregation to grain boundaries and dislocation cores would be the strongest contributor to the increase in the work hardening rate [16, 28, 29]. In fact, activated $\langle c+a \rangle$ dislocations motion is disrupted by the lattice distortions induced by solute atoms and possibly Mg-RE precipitates that were rarely observed in this study. Yin *et al.* demonstrated that RE additions have negligible effect on stacking fault energy (SFE) of basal faults and the energy barrier for transition of pyramidal II stacking faults to basal ones [30]. This observation substantiates the reasoning based on the paramount effects of interfaces/solute atoms and dislocations interactions, as RE additions barely alter dislocation cross slip events [30]. Atop of solute effects, dislocation transmutation events [5, 31] took place with higher frequency in Mg-RE alloys during $\{10\bar{1}2\}$

twin growth, which further enhanced their work hardening rate, particularly compared with pure Mg. This remarkable difference may be associated with two microstructural observations:

1) $\{10\bar{1}2\}$ twins pass across the low angle grain boundaries (LAGBs) between the pancake shaped grains (Figure 3a and b), which resulted in the formation of large twins (Figure 3a and 4a). On the other hand, length of $\{10\bar{1}2\}$ twins are pinned by grain boundaries in pure Mg, which limits their growth. Therefore, in Mg-RE alloys, there is a higher probability of interactions between LAGB dislocations and twin boundaries, which may lead to a higher dislocation forest hardening during early stages of plastic deformation in Region II (i.e. $\varepsilon_t = 0.06 - 0.09$).

2) EBSD scans with 0.1 μm step size in Figure 3c revealed that the transmutation of basal to prismatic dislocations take place during the growth of a $\{10\bar{1}2\}$ twin, which has crossed LAGBs ($< 5°$) composed of geometrically necessary dislocations (GNDs). Figure 3c shows that arrays of basal dislocations that form a LAGB (indicated by red arrows) transmute into prismatic dislocations (indicated by black arrows) as the $\{10\bar{1}2\}$ twin consumes the parent grain [32]. The observed dislocation transmutation enhances the forest hardening rate by producing prismatic dislocations, which have higher CRSS value compared to basal ones [2]. Transmuted prismatic dislocation could serve as hard obstacles for glide of $\langle c + a \rangle$ dislocations within hard orientations.

It is worth noting that the misorientation axis of LAGBs ranging (5-10º) altered from $\langle 10\bar{1}0 \rangle$ to [0001], which is associated with lattice rotations induced by a $\{10\bar{1}2\}$ twin crossing the LAGBs (Figure 3b). Solute segregation to the mentioned boundaries and the transmuted dislocation cores may change their resistance as obstacles for dislocation motion [16].

$\langle c + a \rangle$ dislocations glide rotates twinned lattice around its Taylor axis (i.e. $\langle \bar{1}100 \rangle$) [16], which deviates $\langle c \rangle$-axis of the crystals from compression direction. At $\varepsilon_t = 0.09$, 0.1 μm step size EBSD scan of Mg-0.40 Ce wt. % alloy indicated lattice rotations about 2-6º, which tallies a Schmid factor of 0.04-0.1 for basal slip (Figure 4b).

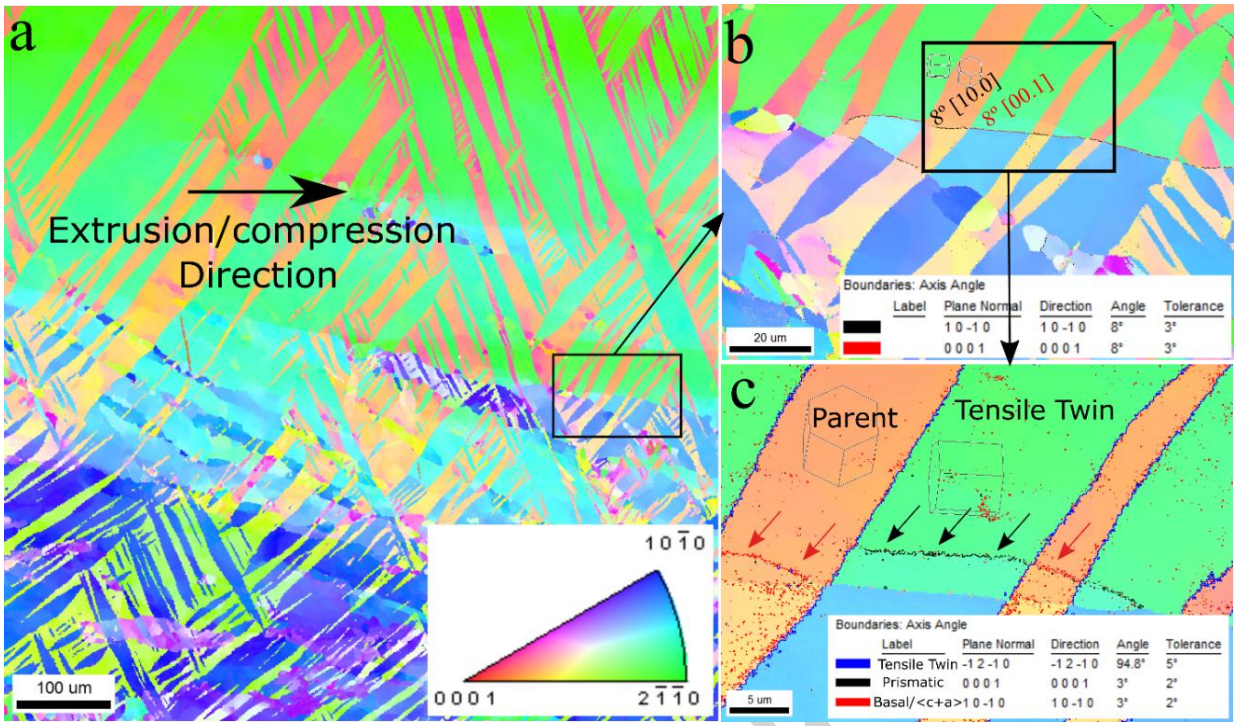

Figure 3. a) A typical EBSD scan of the extruded Mg-0.38 wt. % Gd alloy after compression to 0.04 true strain. Extrusion was performed at 450 ºC with 10 mm/min ram speed. **b)** An IPF map with scanning step size of 0.1 µm illustrating $\{10\bar{1}2\}$ twins passing the grain boundaries. **c)** A higher magnification image from ***b*** highlighting $\{10\bar{1}2\}$ twin boundaries along with basal and prismatic dislocations. Red and black arrows indicate the transmutation of basal to prismatic dislocations as the $\{10\bar{1}2\}$ twins grow.

This boosts the activity of basal and prismatic modes, and the work hardening rate starts to sharply decrease at the beginning of Region III ($\varepsilon_t = 0.09$ till failure), which is conceivably due to the dominance of basal slip with smaller critical resolved shear stress (CRSS) values than $\langle c + a \rangle$ mode [1]. In other words, at $\varepsilon_t = 0.09$, work hardening curves approach their peak values. Region III for pure Mg starts with a smoother transition in hardening behavior, and reaches its peak hardening rate at higher strains, which insinuates less $\langle c + a \rangle$ driven rotations (Figure 2b). $\langle 11\bar{2}0 \rangle || ED$ texture component in pure Mg may also affect the twin saturation strain/behavior due to its lower Schmid factor during extrusion [23, 33]. However, a stark comparison between only binary Mg-RE alloys express a systematic trend of increase in twinning induced work hardening with increasing the RE concentration.

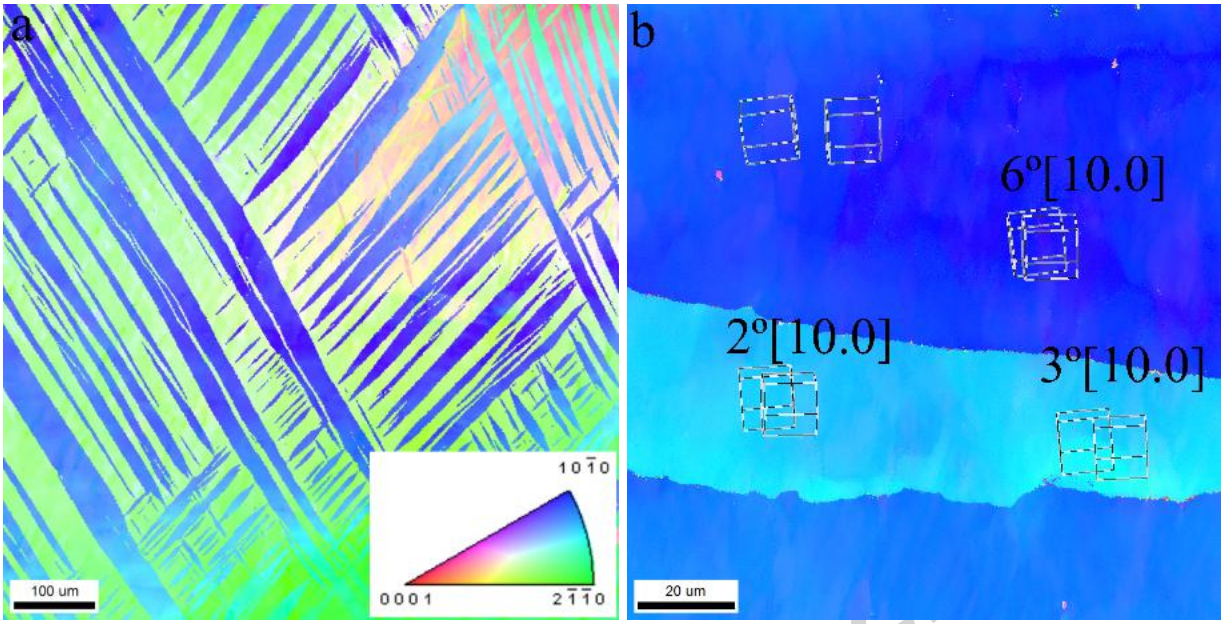

Figure 4. a) A typical EBSD scan of Mg-0.40 wt. % Ce alloy extruded with 10 mm/min ram speed, after compression to 0.04 true strain showing formation of large $\{10\bar{1}2\}$ twins crossing grain boundaries. b) 0.1 µm step size EBSD scan of Mg-0.40 wt. % Ce alloy at $\varepsilon_t = 0.09$ indicating rotations around $\langle 10\bar{1}0 \rangle$ axis within twinned grains.

Figure 5a shows extensive activity of $\{10\bar{1}2\}$ twins in pure magnesium at $\varepsilon_t = 0.04$, which consume nearly all the parent grains at $\varepsilon_t = 0.09$ (Figure 2a). This leads to higher stored strain energy and deformation inhomogeneity at grain boundaries and triple junctions, which triggers low temperature dynamic recrystallization (LTDRX) at room temperature. Figure 5b demonstrates the nucleation of DRX at triple junctions, which have the highest local energy, to produce fresh DRX grains for continuation of plastic deformation. Occurrence of LTDRX is substantiated by refinement of the average grain size from 41 to 12 µm. However, small additions of RE halts recrystallization nucleation at room temperature due to recrystallization retardation [12, 24]. We propose that LTDRX causes a smooth transition of dislocation activities, while Region III starts sharply for Mg-RE alloys in the absence of restoration phenomena.

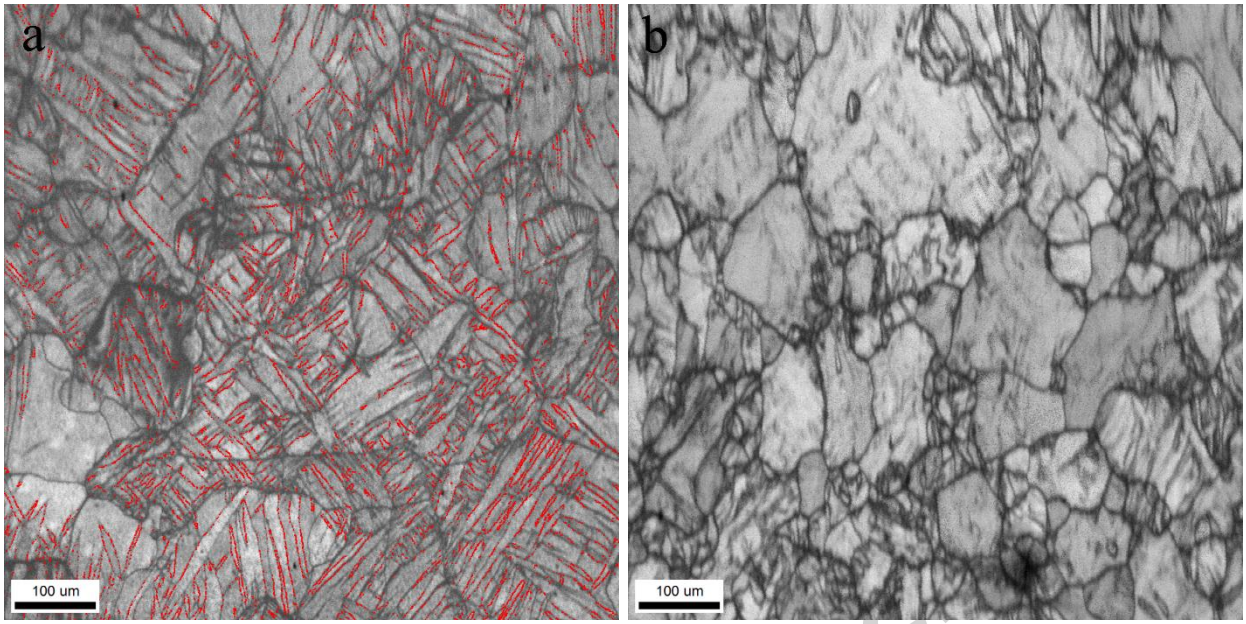

Figure 5. Image quality (IQ) map of extruded pure Mg strained to **a)** true strain of 0.02 showing the immense activity of $\{10\bar{1}2\}$ twinning (highlighted in red) within the relatively coarse grains of extruded pure Mg, **b)** true strain of 0.09 revealing the occurrence of low temperature dynamic recrystallization upon twin saturation, wherein average grain size drops from 41 to 12 μm.

4. Summary and conclusions

We investigated the effect of RE element additions on hardening typically associated with $\{10\bar{1}2\}$ twinning. Our mechanical testing results indicated a notable increase in work hardening rate in RE element containing alloys, which boosted their plastic flow stress. Our micro-texture analyses clearly supported the test results. While in these alloys $\{10\bar{1}2\}$ twins nucleated shortly after the yield point and swiftly traversed low angle grain boundaries, in pure Mg, grain boundaries stopped twin propagation. This resulted in formation of large $\{10\bar{1}2\}$ twins in Mg-RE alloys that enhanced the interaction of grain boundary dislocations and twin boundaries. Moreover, transmutation of basal $\langle a \rangle$ to prismatic $\langle a \rangle$ dislocations occurred during growth of the twins that crossed several low angle grain boundaries. Upon twin saturation, RE element additions boosted $\langle c + a \rangle$ dislocations activity, which significantly enhanced the work hardening rate due to solute drag events and entanglement with transmuted prismatic dislocation. High work hardening rate more than compensated for the softer $\langle c + a \rangle$ slip in RE containing alloys and yielded higher flow stress. $\langle c + a \rangle$ activity within hard orientations induced rotations

around the $\langle \bar{1}100 \rangle$ Taylor axis which boosted basal $\langle a \rangle$ slip. Higher basal $\langle a \rangle$ slip resulted in a sharp drop in the work hardening rate of RE element containing alloys.

Acknowledgment

All the experimental work of this research was conducted in Center for Advanced Vehicular Systems (CAVS) at Mississippi State University. This research was sponsored by the Army Research Laboratory and was accomplished under Cooperative Agreement Number W911NF-15-2-0025. The views and conclusions contained in this document are those of the authors and should not be interpreted as representing the official policies, either expressed or implied, of the Army Research Laboratory or the U.S. Government. The U.S. Government is authorized to reproduce and distribute reprints for Government purposes notwithstanding any copyright notation herein.

References

[1] S.R. Agnew, Ö. Duygulu, Plastic anisotropy and the role of non-basal slip in magnesium alloy AZ31B, Int. J. Plast. 21(6) (2005) 1161-1193.
[2] A. Imandoust, C. Barrett, T. Al-Samman, K. Inal, H. El Kadiri, A review on the effect of rare-earth elements on texture evolution during processing of magnesium alloys, J. Mater. Sci. 52(1) (2017) 1-29.
[3] H. El Kadiri, J. Kapil, A. Oppedal, L. Hector, S.R. Agnew, M. Cherkaoui, S. Vogel, The effect of twin–twin interactions on the nucleation and propagation of twinning in magnesium, Acta Mater. 61(10) (2013) 3549-3563.
[4] A. Jain, S. Agnew, Modeling the temperature dependent effect of twinning on the behavior of magnesium alloy AZ31B sheet, Mater. Sci. Eng. A 462(1) (2007) 29-36.
[5] H. El Kadiri, A. Oppedal, A crystal plasticity theory for latent hardening by glide twinning through dislocation transmutation and twin accommodation effects, J. Mech. Phys. Solids 58(4) (2010) 613-624.
[6] S.-G. Hong, S.H. Park, C.S. Lee, Role of {10–12} twinning characteristics in the deformation behavior of a polycrystalline magnesium alloy, Acta Mater. 58(18) (2010) 5873-5885.
[7] M. Barnett, Twinning and the ductility of magnesium alloys: Part II."Contraction" twins, Mater. Sci. Eng. A 464(1) (2007) 8-16.
[8] I. Beyerlein, J. Wang, M. Barnett, C. Tomé, Double twinning mechanisms in magnesium alloys via dissociation of lattice dislocations, Proc. R. Soc. A, The Royal Society, 2012, pp. 1496-1520.
[9] J.P. Hadorn, K. Hantzsche, S. Yi, J. Bohlen, D. Letzig, S.R. Agnew, Effects of Solute and Second-Phase Particles on the Texture of Nd-Containing Mg Alloys, Metall. Mater. Trans. A 43(4) (2012) 1363-1375.
[10] K. Hantzsche, J. Bohlen, J. Wendt, K.U. Kainer, S.B. Yi, D. Letzig, Effect of rare earth additions on microstructure and texture development of magnesium alloy sheets, Scripta Mater. 63(7) (2010) 725-730.
[11] N. Stanford, M.R. Barnett, The origin of "rare earth" texture development in extruded Mg-based alloys and its effect on tensile ductility, Mater. Sci. Eng. A 496(1-2) (2008) 399-408.
[12] R. Cottam, J. Robson, G. Lorimer, B. Davis, Dynamic recrystallization of Mg and Mg–Y alloys: Crystallographic texture development, Mater. Sci. Eng. A 485(1-2) (2008) 375-382.
[13] J. Bohlen, S. Yi, D. Letzig, K.U. Kainer, Effect of rare earth elements on the microstructure and texture development in magnesium–manganese alloys during extrusion, Mater. Sci. Eng. A 527(26) (2010) 7092-7098.

[14] N. Stanford, Micro-alloying Mg with Y, Ce, Gd and La for texture modification—A comparative study, Mater. Sci. Eng. A 527(10-11) (2010) 2669-2677.
[15] C.D. Barrett, A. Imandoust, A.L. Oppedal, K. Inal, M.A. Tschopp, H. El Kadiri, Effect of grain boundaries on texture formation during dynamic recrystallization of magnesium alloys, Acta Mater. 128 (2017) 270-283.
[16] J.P. Hadorn, K. Hantzsche, S. Yi, J. Bohlen, D. Letzig, J.A. Wollmershauser, S.R. Agnew, Role of Solute in the Texture Modification During Hot Deformation of Mg-Rare Earth Alloys, Metall. Mater. Trans. A 43(4) (2011) 1347-1362.
[17] A. Jain, O. Duygulu, D. Brown, C. Tomé, S. Agnew, Grain size effects on the tensile properties and deformation mechanisms of a magnesium alloy, AZ31B, sheet, Mater. Sci. Eng. A 486(1) (2008) 545-555.
[18] M. Barnett, Z. Keshavarz, A. Beer, D. Atwell, Influence of grain size on the compressive deformation of wrought Mg–3Al–1Zn, Acta Mater. 52(17) (2004) 5093-5103.
[19] B. Clausen, C. Tomé, D. Brown, S. Agnew, Reorientation and stress relaxation due to twinning: modeling and experimental characterization for Mg, Acta Mater. 56(11) (2008) 2456-2468.
[20] J. Koike, Enhanced deformation mechanisms by anisotropic plasticity in polycrystalline Mg alloys at room temperature, Metall. Mater. Trans. A 36(7) (2005) 1689-1696.
[21] M.D. Nave, M.R. Barnett, Microstructures and textures of pure magnesium deformed in plane-strain compression, Scripta Mater. 51(9) (2004) 881-885.
[22] M.R. Barnett, Twinning and the ductility of magnesium alloys, Mater. Sci. Eng. A 464(1-2) (2007) 1-7.
[23] D.W. Brown, S.R. Agnew, M.A.M. Bourke, T.M. Holden, S.C. Vogel, C.N. Tomé, Internal strain and texture evolution during deformation twinning in magnesium, Mater. Sci. Eng. A 399(1-2) (2005) 1-12.
[24] J.P. Hadorn, R.P. Mulay, K. Hantzsche, S. Yi, J. Bohlen, D. Letzig, S.R. Agnew, Texture Weakening Effects in Ce-Containing Mg Alloys, Metall. Mater. Trans. A 44(3) (2012) 1566-1576.
[25] S. Sandlöbes, M. Friák, J. Neugebauer, D. Raabe, Basal and non-basal dislocation slip in Mg–Y, Mater. Sci. Eng. A 576 (2013) 61-68.
[26] S.R. Agnew, L. Capolungo, C.A. Calhoun, Connections between the basal I1 “growth” fault and 〈c+a〉 dislocations, Acta Mater. 82 (2015) 255-265.
[27] S. Sandlöbes, S. Zaefferer, I. Schestakow, S. Yi, R. Gonzalez-Martinez, On the role of non-basal deformation mechanisms for the ductility of Mg and Mg–Y alloys, Acta Mater. 59(2) (2011) 429-439.
[28] N. Stanford, D. Atwell, A. Beer, C. Davies, M.R. Barnett, Effect of microalloying with rare-earth elements on the texture of extruded magnesium-based alloys, Scripta Mater. 59(7) (2008) 772-775.
[29] J. Nie, Y. Zhu, J. Liu, X.-Y. Fang, Periodic segregation of solute atoms in fully coherent twin boundaries, Science 340(6135) (2013) 957-960.
[30] B. Yin, Z. Wu, W. Curtin, First-principles calculations of stacking fault energies in Mg-Y, Mg-Al and Mg-Zn alloys and implications for< c+ a> activity, Acta Mater. (2017).
[31] A. Oppedal, H. El Kadiri, C. Tomé, G. Kaschner, S.C. Vogel, J. Baird, M. Horstemeyer, Effect of dislocation transmutation on modeling hardening mechanisms by twinning in magnesium, Int. J. Plast. 30 (2012) 41-61.
[32] A. Serra, D. Bacon, Computer simulation of screw dislocation interactions with twin boundaries in HCP metals, Acta metallurgica et materialia 43(12) (1995) 4465-4481.
[33] A. Imandoust, C.D. Barrett, A.L. Oppedal, W.R. Whittington, Y. Paudel, H. El Kadiri, Nucleation and preferential growth mechanism of recrystallization texture in high purity binary magnesium-rare earth alloys, Acta Mater. 138 (2017) 27-41.